Noninvasive diagnosis of vulnerable coronary plaque

Eduardo Pozo, Pilar Agudo-Quilez, Antonio Rojas-González, Teresa Alvarado, María José Olivera, Luis Jesús Jiménez-Borreguero, Fernando Alfonso

Eduardo Pozo, Pilar Agudo-Quilez, Antonio Rojas-González, Teresa Alvarado, Luis Jesús Jiménez-Borreguero, Fernando Alfonso, Cardiology Department, Hospital Universitario de La Princesa, IIS-IP, Universidad Autónoma de Madrid, 28006 Madrid, Spain

María José Olivera, Radiology Department, Hospital Universitario de La Princesa, IIS-IP, Universidad Autónoma de Madrid, 28006 Madrid, Spain

Luis Jesús Jiménez-Borreguero, Centro Nacional de Investigaciones Cardiovasculares, 28029 Madrid, Spain

Abstract

Myocardial infarction and sudden cardiac death are frequently the first manifestation of coronary artery disease. For this reason, screening of asymptomatic coronary atherosclerosis has become an attractive field of research in cardiovascular medicine. Necropsy studies have described histopathological changes associated with the development of acute coronary events. In this regard, thin-cap fibroatheroma has been identified as the main vulnerable coronary plaque feature. Hence, many imaging techniques, such as coronary computed tomography, cardiac magnetic resonance or positron emission tomography, have tried to detect noninvasively these histomorphological characteristics with different approaches. In this article, we review the role of these diagnostic tools in the detection of vulnerable coronary plaque with particular interest in their advantages and limitations as well as the clinical implications of the derived findings.

Key words: Atherosclerosis; Vulnerable coronary plaque; Diagnosis; Cardiac computed tomography; Cardiac magnetic resonance

Core tip: Noninvasive diagnosis of vulnerable coronary plaque has become of major interest in preventive cardiology. Certain histological features have been related with an increased risk of plaque rupture. Coronary computed tomography has been largely used for this aim, and some lesion characteristics have been consistently associated with acute coronary syndrome

in several studies. Moreover, a growing body of evidence suggests the potential role of cardiac magnetic resonance and positron emission tomography in high-risk lesion detection. These promising results should be put in perspective to select the high-risk population that may benefit the most from the use of coronary vulnerable plaque imaging screening.

INTRODUCTION

Atherosclerosis constitutes the leading cause of morbidity and mortality in the developed countries, mostly secondary to acute coronary syndromes (ACS)[1]. Moreover, the progressive aging of the population forecasts an exponential growth of the prevalence of cardiovascular disease[2]. In this clinical scenario, detection of patients at risk of suffering an ACS has become one of the major goals in cardiology. Traditional cardiovascular risk factors have been extensively used for this aim. Nevertheless, they fail to anticipate the occurrence of an ACS, especially in certain populations[3,4], so myocardial infarction and sudden cardiac death (SCD) are frequent first manifestations of coronary disease. This situation has boosted the interest in subclinical detection of atherosclerosis. In this regard, quantification of calcium score with coronary computed tomography (CCT)[5] as well as ultrasound evaluation of carotid atherosclerosis[6,7] have demonstrated their utility for cardiovascular risk reclassification[8,9]. In any case, in spite of a very common detection of coronary atherosclerosis in autopsy series among young adults[10] the incidence of ACS in this population is very low[1]. Thus, the onus should be shifted onto the detection of lesions that are prone to develop a coronary event.

VULNERABLE CORONARY PLAQUE: DEFINITION, HISTOPATHOLOGICAL FEATURES AND RATIONALE FOR NONINVASIVE DIAGNOSIS

Classical studies supported that ACS were caused mainly by lesions with severe stenosis[11]; however, PROSPECT trial[12], a prospective intravascular ultrasound (IVUS) and virtual histology (VH) follow-up of non-culprit lesions after ACS, revealed that most of the events are derived from angiographically mild stenosis (< 50%). Again autopsy studies have provided relevant information regarding the atherosclerotic plaque characteristics in culprit lesions. The most frequent presentation is plaque rupture, followed by plaque erosion[13]. Rarely (2%-7% of the cases) the ACS are related with a calcified nodule morphology[14]. These lesions are unfailingly associated with a variable amount of thrombus[15]. Given that plaque rupture is the most common substrate of acute coronary events, vulnerable plaques are defined as lesions at the greatest risk of rupture, with subsequent thrombosis or rapid stenosis progression (Table 1)[16]. Therefore, they are also named high-risk or thrombosis-prone plaques.

When ruptured plaques leading to acute coronary events were studied in necropsies, they usually presented a large necrotic core with a thin overlying fibrous cap together with inflammatory cells and little calcification[17]. Moreover, unlike lesions related to stable disease, these plaques showed expansive or positive remodeling not causing significant narrowing of the coronary lumen[18]. Thus, plaques with these histomorphologic features but intact fibrous cap, named thin-cap fibroatheroma (TCFA), were assumed to be prone to rupture. This concept was evaluated in a detailed histologic analysis of atherosclerotic plaques from a large series of patients who suffered SCD[19]. This study established a relevance hierarchy of morphological features that may influence plaque rupture. In a general analysis a thin fibrous cap (< 84 μm) was able to exclude stable lesions. Interestingly, among TCFA with a cap thickness < 54 μm cross-section area stenosis was most likely < 74%. Finally, when fibrous cap thickness was not considered in the analysis, inflammation, characterized by macrophage plaque infiltration, as well as a large necrotic core emerged as typical features of potentially unstable lesions. In this regard, aforementioned PROSPECT trial[12] was able to confirm these findings *in vivo* with IVUS. In this study plaque burden ≥ 70%, minimal luminal area ≤ 4 mm^2 and TCFA characteristics on VH were independently associated with subsequent major adverse cardiovascular events (MACE) derived from non-culprit lesions.

Some considerations should be kept in mind to understand the clinical relevance of vulnerable plaque detection. All the plaque ruptures do not inevitably cause an ACS[20], whereas disruption and healing is the typical mechanism of plaque stenosis growth[21,22]. Thus, a perfect storm scenario, with confluence of plaque vulnerability, inflammatory state, platelet activation and impaired fibrinolysis, is necessary for ACS occurrence[23]. However, given that substrate presence is a *conditio sine qua non* and the other involved factors (homeostasis disbalance and thrombogenicity) are difficult to establish and/or variable in time, noninvasive detection of vulnerable plaques may be clinically relevant[24], especially in very high risk patients[25].

Hence, in this paper we review the different noninvasive diagnostic tools to evaluate vulnerable coronary plaques, with a detailed description of the relevant information they provide as well as their particular strengths and limitations (Table 2). We focus specially

| Table 1 Concepts related to vulnerable coronary plaque[16]	
Culprit lesion	Coronary lesion considered to be responsible for the clinical event, usually plaque complicated by intraluminal thrombosis
Thrombosed plaque	Plaque with an overlying thrombus extending into the vessel lumen either occlusive or non-occlusive
Eroded plaque	Thrombosed plaque (mainly fibrotic or proteoglycan-rich) due to loss or dysfunction of endothelial cells without associated rupture
Plaque with calcified nodule	Heavily calcified protruding plaque with loss or dysfunction of endothelial cells
Vulnerable, high-risk or thrombosis prone plaque	Plaque at increased risk of thrombosis and rapid stenosis progression TCFA: Inflamed plaque with a thin cap covering a lipid-rich necrotic core
Vulnerable patient	Patient at high-risk to experience a cardiovascular ischemic event due to a high atherosclerotic burden, high-risk plaques and/or thrombogenic blood

TCFA: Thin-cap fibroatheroma.
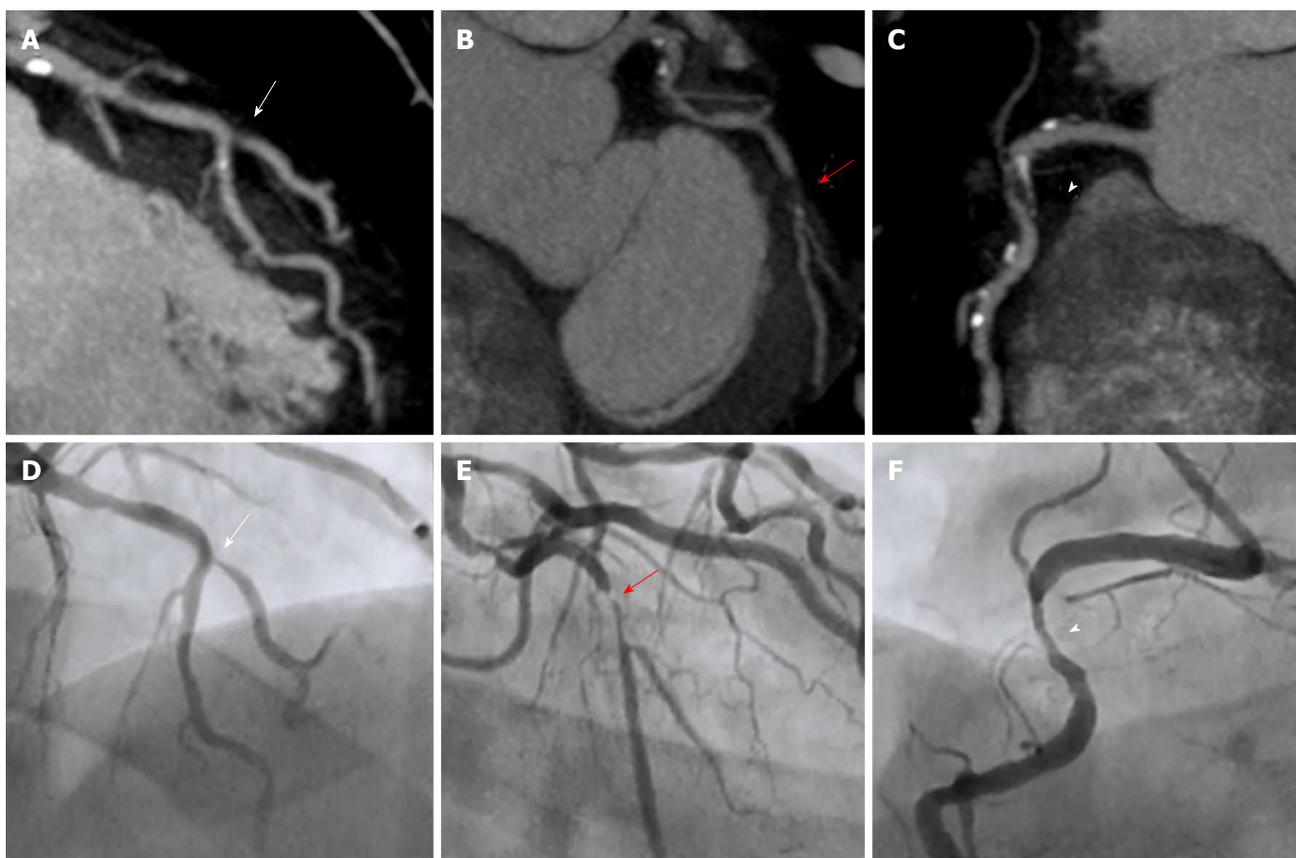
Figure 1 Coronary computed tomography stenosis evaluation compared with invasive coronary angiography. Case of a patient with 3-vessel disease. Maximum intensity projection CCT findings are shown in the upper row with the corresponding ICA projections in the lower row. (A) demonstrates a significant stenosis in the ostium of the diagonal branch (arrow) at the level of its take-off from the mid-LAD in both CCT and ICA (D); In (B) CCT shows a subtotal occlusion in the proximal LCx (red arrow) that corresponds to a critical lesion at the same level in ICA (E); In CCT image from (C) a mixed plaque is detected in proximal RCA causing a significant stenosis (arrowhead), as corroborated by ICA (F). CCT: Coronary computed tomography; ICA: Invasive coronary angiography; LAD: Left anterior descending coronary artery; LCx: Left circumflex coronary artery; RCA: Right coronary artery.

on the technique with the greatest evidence in this field, CCT, mentioning other available imaging tools with promising perspective such as cardiac magnetic resonance (CMR) imaging and positron emission tomography (PET).

CCT

CCT general information with predictive value

CCT not only provides information about the presence of significant stenoses with a high diagnostic accuracy[26] (Figure 1) but also allows a sensitive noninvasive direct evaluation of coronary atherosclerosis[27]. Coronary calcium score determination[28] as well as non-calcified plaque detection, even in the absence of significant stenosis[29-31], have demonstrated their value to predict MACE. Moreover, a large and systematic meta-analysis highlighted the relevance of luminal stenosis severity assessment with CCT[32], showing an increasing risk of the composite end-point of cardiac death or myocardial
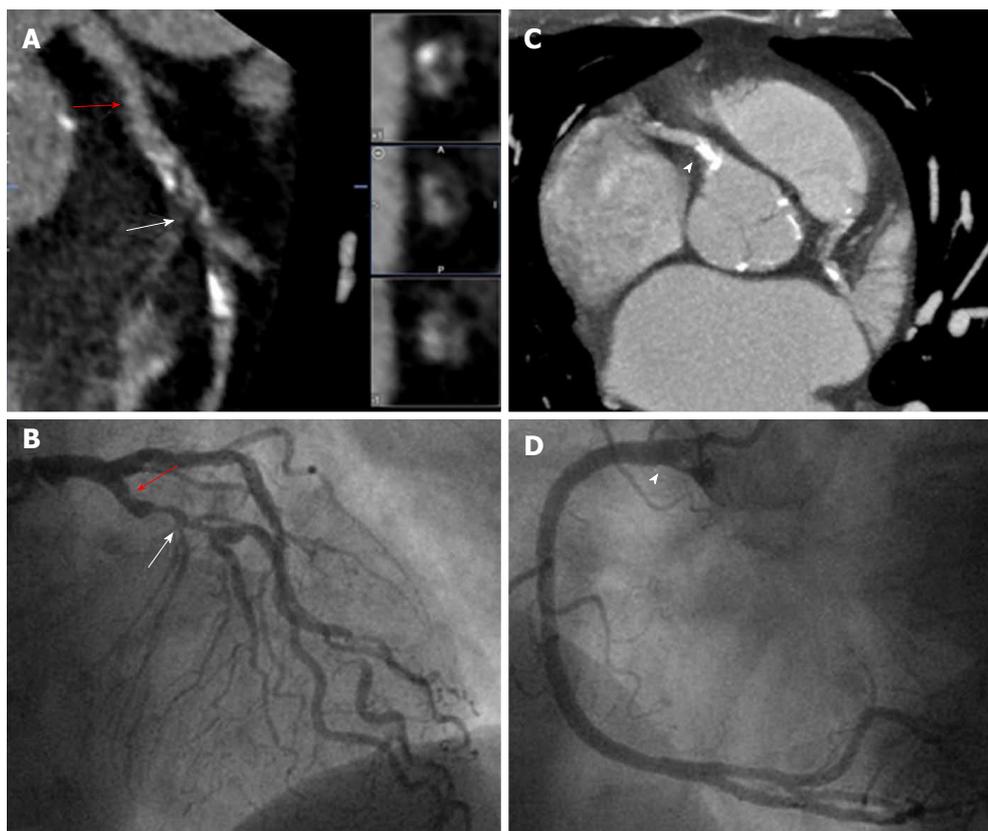
Figure 2 Coronary plaque categories by coronary computed tomography. Patient with chest pain referred for CCT. A: LAD in multiplanar reconstruction with a mixed plaque in the mid segment (arrow) that causes significant stenosis confirmed in the ICA (B, arrow). Note that there is also a nonsignificant noncalcified plaque in the proximal segment (red arrow) that is barely seen in coronariography (B, red arrow); C: A maximum intensity projection that demonstrates a severely calcified plaque in the ostial RCA (arrowhead), which does not allow luminal stenosis evaluation. However, ICA (D) confirms the absence of significant stenosis at the same level (arrowhead). CCT: Coronary computed tomography; LAD: Left anterior descending coronary artery; ICA: Invasive coronary angiography; RCA: Right coronary artery.

Table 2 Diagnostic tests for noninvasive evaluation of coronary vulnerable plaque

	CCT	CMR	PET
Plaque characterization	Plaque morphology	Plaque morphology Tissue characterization of plaque	Inflammation (FDG) Macrophage infiltration (new tracers)
Vulnerable features	Positive remodeling Low attenuation Spotty calcification Napkin-ring sign	Positive remodeling T1 hyperintensity Late gadolinium enhancement	Increased tracer uptake
Clinical relevance	Strong association with ACS Prediction of slow-flow after PCI Evaluation of response to statins	Initial data of association of T1 hyperintense plaques with slow-flow, ACS and response to statins	Differentiation between ACS and stable coronary disease
Limitations	Radiation exposure Heavy calcification Overlap in attenuation ranges Inability to detect plaque erosion	Direct relation between spatial resolution and acquisition time Susceptibility to motion artifacts	Low spatial and temporal resolution Myocardial background uptake Expensive and limited availability

CCT: Coronary computed tomography; CMR: Cardiac magnetic resonance; PET: Positron emission tomography; ACS: Acute coronary syndrome; PCI: Percutaneous coronary intervention; FDG: Fluorodeoxyglucose.

infarction for absence (0.04%), non-obstructive (1.29%) and obstructive (6.53%) coronary artery disease. It has shown a particular utility in chest pain evaluation at the emergency room[33]. There is also data supporting the capacity of CCT to evaluate coronary anatomy to determine the best revascularization strategy[34].

Coronary plaque characterization with CCT
Certainly, the most relevant information is derived from the direct evaluation of coronary plaque with CCT. By consensus[35] the lesions are classified in 3 categories: Non-calcified, calcified and mixed plaques (Figure 2). In this regard, for a further assessment of CCT
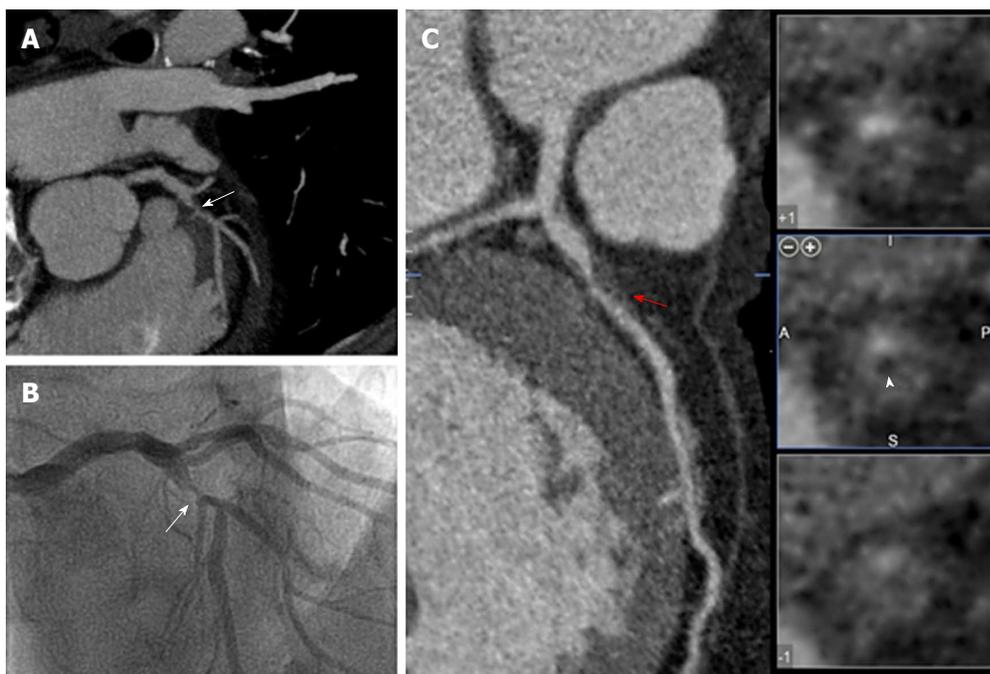
Figure 3 Vulnerable coronary plaque features by coronary computed tomography. Patient with unstable angina who underwent CCT followed by ICA. A severe stenosis (arrows) in mid-LAD just before the origin of the second diagonal was detected in CCT (A) and subsequently confirmed by ICA (B); A detailed analysis of multiplanar reconstruction of CCT (C) revealed the presence of positive remodeling (red arrow) and low attenuation (arrow head) at the level of the culprit lesion, both signs associated with vulnerable coronary plaque. CCT: Coronary computed tomography; ICA: Invasive coronary angiography; LAD: Left anterior descending coronary artery.

accuracy in coronary plaque qualitative analysis, head-to-head comparisons with VH have been performed. Pundziute *et al*[36] found a good correlation between both diagnostic tools in plaque characterization, with more fibrotic and fibro-fatty components in non-calcified plaque. Besides, the majority of TCFA in IVUS corresponded to mixed plaques in CCT. Hereof, Choi *et al*[37] established that plaques with > 10% necrotic core by VH showed significantly lower HU values in CCT. All the studies have shown a good agreement in non-calcified plaque quantification between both techniques[38-40]. However, there were contradictory results in plaque composition analysis using predefined Hounsfield unit (HU) ranges, due to overlapping in these values[38,40]. On the other hand, optical coherence tomography (OCT) has also been used as reference intravascular imaging technique. Kashiwagi *et al*[41] divided plaques in TCFA and non-TCFA according to OCT findings and studied the CCT plaque characteristics. Positive remodeling, lower attenuation values and ring-like enhancement (napkin-ring sign) on CCT were significantly more common in OCT-derived TCFA lesions. The later feature showed a good diagnostic accuracy for high-risk plaque detection and was independently associated with acute events. Moreover, napkin-ring sign has been independently associated with necrotic/lipid core area, non-core plaque area and total vessel area in post-mortem histopathological correlation[42]. However, although the presence of low attenuation and positive remodeling in CCT could identify rupture plaques in another study[43], they failed to differentiate plaque erosions leading to ACS from stable lesions. Lastly, CCT accuracy for plaque composition characterization was also evaluated with near-infrared spectroscopy (NIRS), showing a good correlation of plaque burden and non-calcified plaque area and density with cholesterol deposition in the coronary wall[27].

Thereby, even with first generation 16-rows scanners, culprit lesion characteristics could be evaluated in ACS[44]. When these lesions were compared with those in patients with stable angina, positive expansive remodeling, low attenuation (< 30 HU) non-calcified plaques and spotty calcification were detected more frequently (Figure 3). Furthermore, the combination of these three features increased the positive predictive value to 95%. These findings were corroborated with a prospective multimodal imaging protocol in acute coronary events[45]. Again lower radiological density with lower calcium score and larger remodeling index were more common in culprit lesions. Interestingly, these plaque characteristics were confirmed with IVUS and VH.

Beyond the classical tools for CCT analysis, there are new approaches with promising results in coronary plaque evaluation. Fujimoto *et al*[46] showed that the presence of delayed plaque enhancement in serial CCT acquisition was associated with high-risk plaque features. They hypothesized that this finding may be explained by plaque neovascularization and/or inflammation. In the same direction, a contrast agent formed by iodinated nanoparticles has been probed to detect macrophages in a preclinical model of atherosclerosis[47].

Prognostic relevance of plaque characterization with CCT

The hypothesis that aforementioned morphological patterns are able to identify thrombosis-prone plaques was evaluated in prospective studies. Motoyama *et al*[48] analyzed for the first time CCT plaque characteristics associated with the incidence of ACS in the follow-up. In this study, the presence of positive remodeling and/or low attenuation plaque was independently associated with ACS (HR = 22.8; *P* < 0.001) (Figure 3). Napkin-ring sign is another feature that has been associated with thrombosis-prone plaque. In a large series this sign was the strongest predictor of ACS among the vulnerable plaque characteristics[49]. On the other hand, a case-control study[50] demonstrated that when a semiautomated quantitative analysis of CCT was implemented, total and relative plaque volume and non-calcified plaque were significantly higher in patients who suffered an acute coronary event. This method of evaluation also had additive value to classical cardiovascular risk factors and conventional CCT reading for ACS prediction. Nevertheless, on top of the some methodological limitations[51], there is contradictory results in large prospective series. Among patients derived from ROMICAT II cohort[52], acute chest pain in emergency room, presence of a least one of high risk features (positive remodeling, low attenuation, spotty calcification and napkin-ring sign) was an independent predictor of ACS, even after adjustment by clinical risk factors and > 50% or > 70% stenosis[52]. Conversely, when stable patients were evaluated, plaque feature analysis, although improved predictive accuracy, did not significantly increase model discrimination index for acute coronary events[53]. Interestingly, the relevance of high-risk plaque detection on CCT was analyzed in another important cohort from a patient-based and lesion-based perspective[54]. In the former, vulnerable plaque was independently associated with prognosis. However, presence of high-risk features failed to predict ACS in a lesion-based analysis. Additionally, when serial CCT was available, plaque progression emerged as an independent predictor of events. Putting all these data in perspective, although vulnerable plaque CCT features may predict ACS the clinical relevance of these finding still needs to be clarify.

Influence of CCT plaque characteristics in percutaneous coronary interventions outcome was evaluated as well. The incidence of slow-flow phenomenon in patients with stable coronary disease was related with the presence of circumferential plaque calcification, a higher positive remodeling index and a lower plaque density in previous CCT[55]. In fact, circumferential plaque calcification showed the strongest independent association with this complication.

Finally, when CCT was used to evaluate the response to statin therapy[56] a greater decrease of total plaque volume, due to reduction in low attenuation plaque, was detected among patients under treatment, without differences in lumen volume and remodeling index changes between the groups. Thus, CCT may play a role in evaluation of the response to lipid-lowering drugs.

Limitations of CCT in coronary plaque evaluation

Despite the promising data, CCT is far from be free of limitations in vulnerable coronary plaque analysis. First, precise definition of plaque components is hampered by inherent limited spatial resolution of this imaging technique. Thus, results of non-calcified plaque quantification may be inconsistent[39,57]. Moreover, as previously mentioned, CCT plaque characterization is restricted by the overlap in radiological attenuation ranges for the different types of lesions[58,59] (Figure 4). In this regard, dual-source CCT, whose 2 different energies provide differing attenuation of materials, have shown to improve differentiation of necrotic core and fibrous plaque *ex vivo*[60]. Nevertheless, these results worsened when applied *in vivo*[38,60]. Thus, CCT acquisition technology needs to be refined to establish a generalizable HU-based categorization for accurate evaluation of components of the coronary plaque. Second, heavily calcified plaque may obscure detailed plaque evaluation due to partial volume effect. Finally, as previously mentioned, CCT has failed to detect plaque erosion[43], which constitutes the second more frequent presentation of culprit lesions[13].

CMR

CMR not only allows a precise ventricular volume quantification[61] and myocardial tissue characterization[62,63], but also is able to detect the presence of significant (> 50%) coronary atherosclerosis with similar accuracy than CCT[64,65] (Figure 5). In any case, in CMR spatial resolution is directly proportional to scan time. Thus, the necessary high resolution for coronary imaging carries an inherent increased susceptibility to motion artifacts[66]. The most effective measure to optimize image resolution without affecting artifact susceptibility is to reduce the field of view[67], which is difficult if a whole coronary tree analysis is pursued. Apart from that, several strategies have been implemented to avoid aforementioned limitation: Techniques to accelerate image acquisition[68,69], cardiac[70] and respiratory[71] motion compensation and new sampling methods[72,73]. However, even with the last technical advances a whole-heart coronary CMR angiography still takes at least 5 min[74,75], which limits its translation to clinical practice.

Although the aforementioned limitations make the acquisition challenging, non-contrast black-blood sequences have shown a good correlation with IVUS in luminal area and coronary plaque burden determination[76,77]. Interestingly, methemoglobin produced during clot maturation has the potential of shortening T1 relaxation time, which allows coronary thrombus detection with T1-weighted sequences[78,79]. The diagnostic accuracy of this noninvasive technique was
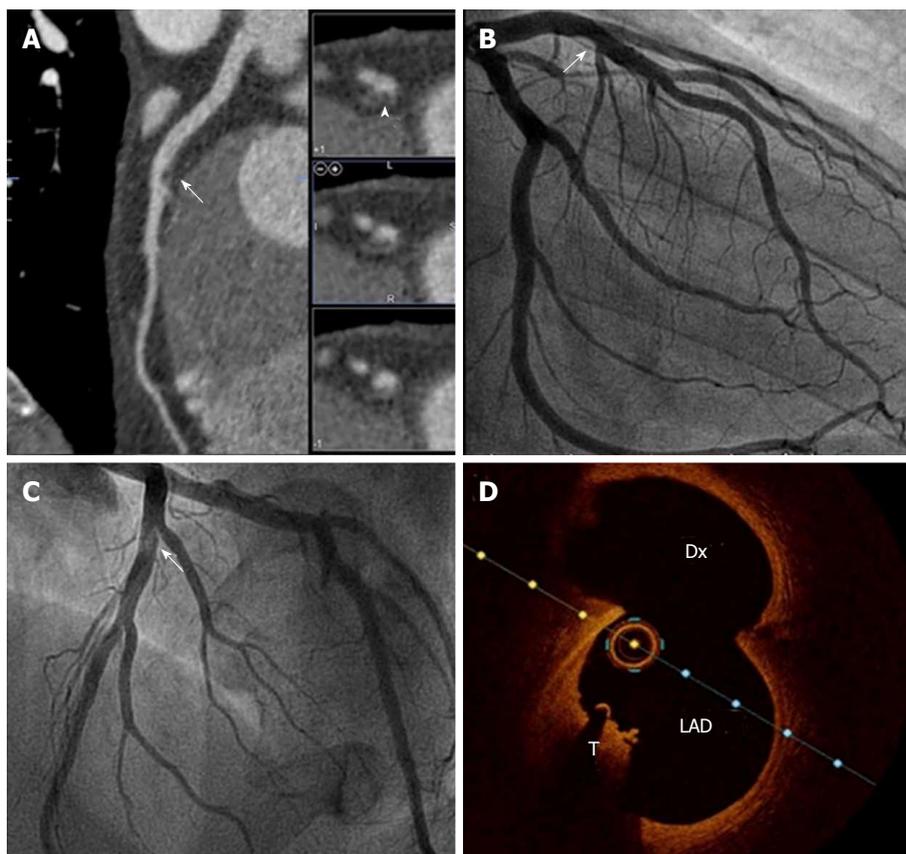
Figure 4 Coronary computed tomography characterization of plaque components. Multimodal evaluation of a mid-LAD lesion in bifurcation with a Dx branch. A: CCT multiplanar reconstruction demonstrates a nonsignificant luminal narrowing in the mid LAD (arrow), and when short axis was evaluated the lesion fulfills noncalcified plaque features (arrowhead); B and C: ICA: The same nonobstructive lesion is observed in mid-LAD (arrow), which seems hyperlucent on LAO cranial projection (C); D: OCT confirms the presence of a red intracoronary thrombus (T) in the same location. CCT: Coronary computed tomography; LAD: Left anterior descending artery; Dx: Diagonal branch; ICA: Invasive coronary angiography; OCT: Optical coherence tomography.

proven to be high when it was evaluated against invasive coronary angiography[80] and OCT[81] (Figure 6). On the other hand, in a head-to-head comparison with CCT the presence of high intensity lesions on T1 sequences was associated with features of vulnerable plaque, such as positive remodeling, low attenuation and spotty calcification[82]. Moreover, this CMR finding was also associated with prognosis: Higher incidence of slow-flow phenomenon after percutaneous coronary intervention[82], coronary events during the follow-up[83], and regression of plaque in response to statin therapy[84]. Finally, T2-weighted sequences have demonstrated their ability to detect coronary vessel wall edema, in probable relation with plaque neovascularization, in initial studies[85,86].

Targeted as well as non-targeted contrast agents have been used to evaluate coronary arteries with CMR. When nonspecific gadolinium contrast is used, the presence of hyperenhancement has been linked to the severity of coronary atherosclerosis[79]. Additionally, a progressive reduction of coronary hyperenhancement has been noted in serial CMR after acute myocardial infarction[87]. Contrarily, many targeted contrast agents, directed to specific components of the plaque, are currently under investigation. Among them some have already reached positive data for coronary evaluation in

large animals and/or humans: Fibrin-specific[88-90] and elastin-specific[91] contrast agents, gadofluorine[92,93], albumin-binding[94-96] contrast agent, and iron oxide-based[97] contrast. However, due to the growing field of molecular imaging a detailed discussion of these agents exceed the scope of this review.

PET

Besides the detailed morphological characterization provided by CCT and CMR, quantification of inflammation is a key feature in vulnerable coronary plaque evaluation. In this regard, nuclear imaging techniques have been extensively used for this purpose in atherosclerosis[98,99]. PET is the preferred tool, due to its superior spatial resolution over single photon emission tomography (SPECT), and is usually combined with computed tomography for a better anatomical definition. Fluorodeoxyglucose (FDG) is the most widely used tracer in this field. However, coronary evaluation is hampered by the significant myocardial uptake of FDG. To override this limitation, free fatty myocardial metabolism was favored with a low-carbohydrate high fat preparation[100]. This strategy was initially proven to detect coronary plaque inflammation[101]. Moreover, when coronary PET was evaluated in ACS as well as in stable angina
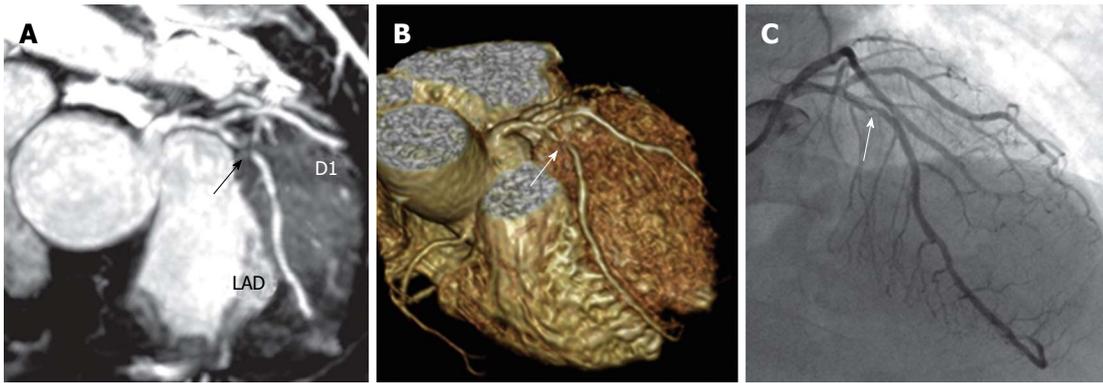
Figure 5 Unenhanced Whole-Heart coronary cardiac magnetic resonance angiography. Correlation of unenhanced whole-heart coronary CMR angiography (A, maximum intensity projection image, and B, volume-rendered image) with invasive coronary angiography (C) in a in a 50-year-old male patient with chest pain on effort. Note the presence of significant stenosis in proximal LAD (arrows). Adapted with permisssion from Nagata *et al*[75]. LAD: Left anterior descending coronary artery; D1: First diagonal branch; CMR: Cardiac magnetic resonance.
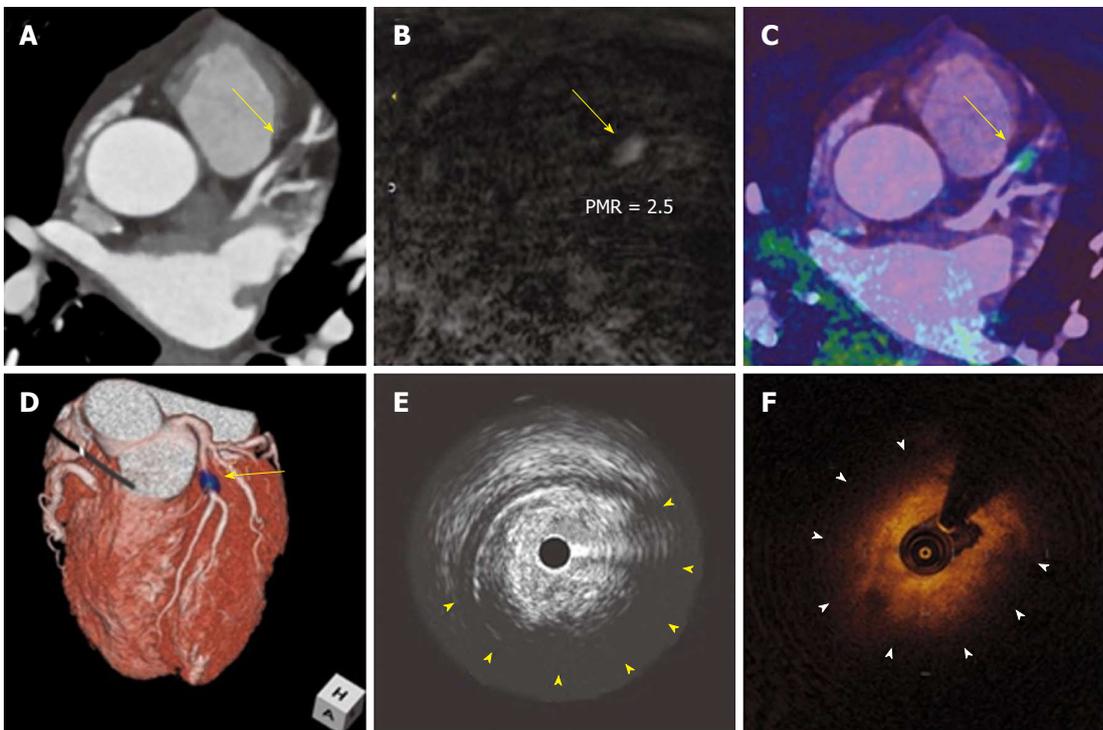

Figure 6 T1 hyperintense coronary plaques in cardiac magnetic resonance. Noninvasive and invasive coronary imaging of a significant plaque in proximal LAD. CCTA (A) showed a noncalcified plaque in LAD causing significant stenosis. When noncontrast T1-weighted CMR imaging was performed (B) a hyperintense lesion was detected. Afterwards, CMR images were fused with CCTA (C and D) and this lesion was found to correspond with the previously described coronary stenosis. Interestingly, during the subsequent coronary angiography it showed a large lipid component in IVUS (E) as well as OCT (F). Adapted with permission from Asaumi *et al*[106]. LAD: Left anterior descending coronary artery; CCTA: Coronary computed tomography; CMR: Cardiac magnetic resonance; IVUS: Intravascular ultrasound; OCT: Optical coherence tomography; PMR: Plaque to myocardium signal intensity ratio.

after stent implantation, a higher FDG uptake was noted not only in the culprit lesions but also in the left main and ascending thoracic aorta of the patients with acute coronary events (Figure 7)[102]. This suggests the presence of spread arterial wall inflammation in the former group. Conversely, Dweck *et al*[103] demonstrated the ability of the new tracer 18F-sodium fluoride to detect coronary atherosclerosis without the limitation of myocardial metabolism artifact. Increased uptake was also associated with coronary calcium score,

Framingham risk score, prior cardiovascular events and angina. Lastly, new tracers targeted against other markers of inflammation such as macrophage infiltration (11C-PK11195[104] and 68Ga-DOTATATE[105]) have been successfully tested.

CONCLUSION

Noninvasive imaging tools have shown their capacity to detect features related with vulnerable coronary
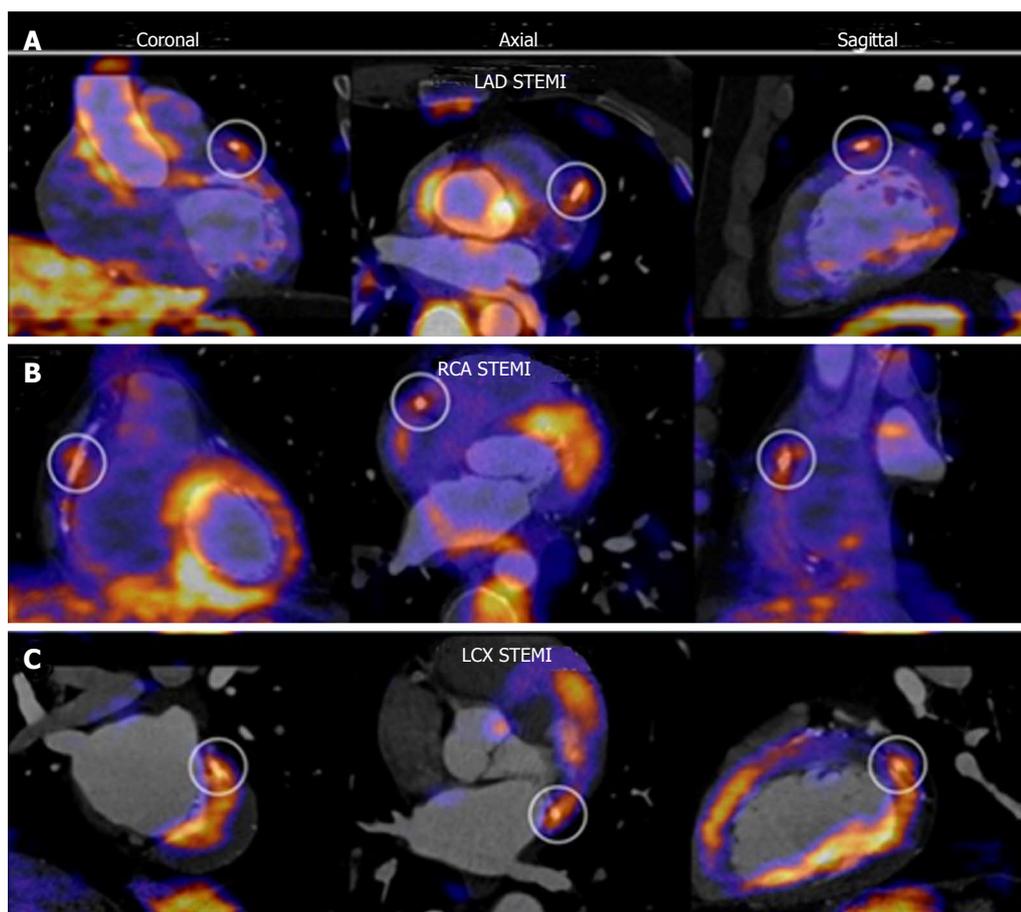
Figure 7 Fluorodeoxyglucose positron emission tomography of the coronary arteries. PET CT fusion imaging in three cases of patients with STEMI. An increased ^{18}F-FDG uptake at stent site is shown in different culprit vessels, from A to C: LAD, RCA and LCX. Adapted with permission from Cheng *et al*[107]. This research was originally published in JNM. ©by the Society of Nuclear Medicine and Molecular Imaging, Inc. FDG: Fluorodeoxyglucose; PET: Positron emission tomography; STEMI: ST elevation myocardial infarction; LAD: Left anterior descending coronary artery; RCA: Right coronary artery; LCX: Left circumflex coronary artery.

plaque. CCT has been largely tested with this aim. Certain plaque characteristics, such as positive remodeling, low attenuation, spotty calcification and napkin-ring sign, have been systematically associated with ACS occurrence. Regarding CMR, results of plaque morphology characterization are similar than CCT but the inherent acquisition limitations hampered its extension to clinical practice. Moreover this technique allows tissue characterization of the coronary plaques through T1- and T2-weighted sequences and contrast-enhanced imaging. Finally, PET has emerged as a promising molecular imaging technique being able to detect coronary inflammation and even macrophage infiltration *in vivo*. In any case, given that the presence of vulnerable plaque features is not irredeemably linked to the occurrence of an ACS, larger studies are needed to clarify the patient subgroup that may benefit from non-invasive detection of high-risk plaques. This aspect is of special interest due to the large population that may be the target of a noninvasive imaging strategy for acute coronary events prevention. In this regard, cost-effectiveness should also be evaluated carefully in the future.

REFERENCES

1   **Mozaffarian D**, Benjamin EJ, Go AS, Arnett DK, Blaha MJ, Cushman M, Das SR, de Ferranti S, Després JP, Fullerton HJ, Howard VJ, Huffman MD, Isasi CR, Jiménez MC, Judd SE, Kissela BM, Lichtman JH, Lisabeth LD, Liu S, Mackey RH, Magid DJ, McGuire DK, Mohler ER, Moy CS, Muntner P, Mussolino ME, Nasir K, Neumar RW, Nichol G, Palaniappan L, Pandey DK, Reeves MJ, Rodriguez CJ, Rosamond W, Sorlie PD, Stein J, Towfighi A, Turan TN, Virani SS, Woo D, Yeh RW, Turner MB. Executive Summary: Heart Disease and Stroke Statistics--2016 Update: A Report From the American Heart Association. *Circulation* 2016; **133**: 447-454 [PMID: 26811276 DOI: 10.1161/CIR.0000000000000366]

2   **Heidenreich PA**, Trogdon JG, Khavjou OA, Butler J, Dracup K, Ezekowitz MD, Finkelstein EA, Hong Y, Johnston SC, Khera A, Lloyd-Jones DM, Nelson SA, Nichol G, Orenstein D, Wilson PW, Woo YJ. Forecasting the future of cardiovascular disease in the United States: a policy statement from the American Heart Association. *Circulation* 2011; **123**: 933-944 [PMID: 21262990 DOI: 10.1161/CIR.0b013e31820a55f5]

3   **Berry JD**, Liu K, Folsom AR, Lewis CE, Carr JJ, Polak JF, Shea S, Sidney S, O'Leary DH, Chan C, Lloyd-Jones DM. Prevalence and progression of subclinical atherosclerosis in younger adults with low short-term but high lifetime estimated risk for cardiovascular disease: the coronary artery risk development in young adults study and multi-ethnic study of atherosclerosis.

Circulation 2009; **119**: 382-389 [PMID: 19139385 DOI: 10.1161/CIRCULATIONAHA.108.800235]

4   **Sibley C**, Blumenthal RS, Merz CN, Mosca L. Limitations of current cardiovascular disease risk assessment strategies in women. *J Womens Health* (Larchmt) 2006; **15**: 54-56 [PMID: 16417419 DOI: 10.1089/jwh.2006.15.54]

5   **Martin SS**, Blaha MJ, Blankstein R, Agatston A, Rivera JJ, Virani SS, Ouyang P, Jones SR, Blumenthal RS, Budoff MJ, Nasir K. Dyslipidemia, coronary artery calcium, and incident atherosclerotic cardiovascular disease: implications for statin therapy from the multi-ethnic study of atherosclerosis. *Circulation* 2014; **129**: 77-86 [PMID: 24141324 DOI: 10.1161/CIRCULATIONAHA.113.003625]

6   **Baber U**, Mehran R, Sartori S, Schoos MM, Sillesen H, Muntendam P, Garcia MJ, Gregson J, Pocock S, Falk E, Fuster V. Prevalence, impact, and predictive value of detecting subclinical coronary and carotid atherosclerosis in asymptomatic adults: the BioImage study. *J Am Coll Cardiol* 2015; **65**: 1065-1074 [PMID: 25790876 DOI: 10.1016/j.jacc.2015.01.017]

7   **Sillesen H**, Muntendam P, Adourian A, Entrekin R, Garcia M, Falk E, Fuster V. Carotid plaque burden as a measure of subclinical atherosclerosis: comparison with other tests for subclinical arterial disease in the High Risk Plaque BioImage study. *JACC Cardiovasc Imaging* 2012; **5**: 681-689 [PMID: 22789936 DOI: 10.1016/j.jcmg.2012.03.013]

8   **Fernández-Friera L**, Peñalvo JL, Fernández-Ortiz A, Ibañez B, López-Melgar B, Laclaustra M, Oliva B, Mocoroa A, Mendiguren J, Martínez de Vega V, García L, Molina J, Sánchez-González J, Guzmán G, Alonso-Farto JC, Guallar E, Civeira F, Sillesen H, Pocock S, Ordovás JM, Sanz G, Jiménez-Borreguero LJ, Fuster V. Prevalence, Vascular Distribution, and Multiterritorial Extent of Subclinical Atherosclerosis in a Middle-Aged Cohort: The PESA (Progression of Early Subclinical Atherosclerosis) Study. *Circulation* 2015; **131**: 2104-2113 [PMID: 25882487 DOI: 10.1161/CIRCULATIONAHA.114.014310]

9   **Naghavi M**, Falk E, Hecht HS, Jamieson MJ, Kaul S, Berman D, Fayad Z, Budoff MJ, Rumberger J, Naqvi TZ, Shaw LJ, Faergeman O, Cohn J, Bahr R, Koenig W, Demirovic J, Arking D, Herrera VL, Badimon J, Goldstein JA, Rudy Y, Airaksinen J, Schwartz RS, Riley WA, Mendes RA, Douglas P, Shah PK. From vulnerable plaque to vulnerable patient--Part III: Executive summary of the Screening for Heart Attack Prevention and Education (SHAPE) Task Force report. *Am J Cardiol* 2006; **98**: 2H-15H [PMID: 16843744 DOI: 10.1016/j.amjcard.2006.03.002]

10 **Nemetz PN**, Roger VL, Ransom JE, Bailey KR, Edwards WD, Leibson CL. Recent trends in the prevalence of coronary disease: a population-based autopsy study of nonnatural deaths. *Arch Intern Med* 2008; **168**: 264-270 [PMID: 18268166 DOI: 10.1001/archinternmed.2007.79]

11 **Ellis S**, Alderman E, Cain K, Fisher L, Sanders W, Bourassa M. Prediction of risk of anterior myocardial infarction by lesion severity and measurement method of stenoses in the left anterior descending coronary distribution: a CASS Registry Study. *J Am Coll Cardiol* 1988; **11**: 908-916 [PMID: 3128587]

12 **Stone GW**, Maehara A, Lansky AJ, de Bruyne B, Cristea E, Mintz GS, Mehran R, McPherson J, Farhat N, Marso SP, Parise H, Templin B, White R, Zhang Z, Serruys PW. A prospective natural-history study of coronary atherosclerosis. *N Engl J Med* 2011; **364**: 226-235 [PMID: 21247313 DOI: 10.1056/NEJMoa1002358]

13 **Virmani R**, Kolodgie FD, Burke AP, Farb A, Schwartz SM. Lessons from sudden coronary death: a comprehensive morphological classification scheme for atherosclerotic lesions. *Arterioscler Thromb Vasc Biol* 2000; **20**: 1262-1275 [PMID: 10807742]

14 **Virmani R**, Burke AP, Farb A, Kolodgie FD. Pathology of the vulnerable plaque. *J Am Coll Cardiol* 2006; **47**: C13-C18 [PMID: 16631505 DOI: 10.1016/j.jacc.2005.10.065]

15 **Kramer MC**, Rittersma SZ, de Winter RJ, Ladich ER, Fowler DR, Liang YH, Kutys R, Carter-Monroe N, Kolodgie FD, van der Wal AC, Virmani R. Relationship of thrombus healing to underlying plaque morphology in sudden coronary death. *J Am Coll Cardiol* 2010; **55**: 122-132 [PMID: 19818571 DOI: 10.1016/j.jacc.2009.09.007]

16 **Schaar JA**, Muller JE, Falk E, Virmani R, Fuster V, Serruys PW, Colombo A, Stefanadis C, Ward Casscells S, Moreno PR, Maseri A, van der Steen AF. Terminology for high-risk and vulnerable coronary artery plaques. Report of a meeting on the vulnerable plaque, June 17 and 18, 2003, Santorini, Greece. *Eur Heart J* 2004; **25**: 1077-1082 [PMID: 15191780 DOI: 10.1016/j.ehj.2004.01.002]

17 **Burke AP**, Farb A, Malcom GT, Liang YH, Smialek J, Virmani R. Coronary risk factors and plaque morphology in men with coronary disease who died suddenly. *N Engl J Med* 1997; **336**: 1276-1282 [PMID: 9113930 DOI: 10.1056/NEJM199705013361802]

18 **Schoenhagen P**, Ziada KM, Kapadia SR, Crowe TD, Nissen SE, Tuzcu EM. Extent and direction of arterial remodeling in stable versus unstable coronary syndromes: an intravascular ultrasound study. *Circulation* 2000; **101**: 598-603 [PMID: 10673250]

19 **Narula J**, Nakano M, Virmani R, Kolodgie FD, Petersen R, Newcomb R, Malik S, Fuster V, Finn AV. Histopathologic characteristics of atherosclerotic coronary disease and implications of the findings for the invasive and noninvasive detection of vulnerable plaques. *J Am Coll Cardiol* 2013; **61**: 1041-1051 [PMID: 23473409 DOI: 10.1016/j.jacc.2012.10.054]

20 **Takano M**, Inami S, Ishibashi F, Okamatsu K, Seimiya K, Ohba T, Sakai S, Mizuno K. Angioscopic follow-up study of coronary ruptured plaques in nonculprit lesions. *J Am Coll Cardiol* 2005; **45**: 652-658 [PMID: 15734606 DOI: 10.1016/j.jacc.2004.09.077]

21 **Burke AP**, Kolodgie FD, Farb A, Weber DK, Malcom GT, Smialek J, Virmani R. Healed plaque ruptures and sudden coronary death: evidence that subclinical rupture has a role in plaque progression. *Circulation* 2001; **103**: 934-940 [PMID: 11181466]

22 **Mann J**, Davies MJ. Mechanisms of progression in native coronary artery disease: role of healed plaque disruption. *Heart* 1999; **82**: 265-268 [PMID: 10455072]

23 **Arbab-Zadeh A**, Nakano M, Virmani R, Fuster V. Acute coronary events. *Circulation* 2012; **125**: 1147-1156 [PMID: 22392862 DOI: 10.1161/CIRCULATIONAHA.111.047431]

24 **Braunwald E**. Noninvasive detection of vulnerable coronary plaques: Locking the barn door before the horse is stolen. *J Am Coll Cardiol* 2009; **54**: 58-59 [PMID: 19555841 DOI: 10.1016/j.jacc.2009.03.040]

25 **Braunwald E**. Epilogue: what do clinicians expect from imagers? *J Am Coll Cardiol* 2006; **47**: C101-C103 [PMID: 16631504 DOI: 10.1016/j.jacc.2005.10.072]

26 **Mowatt G**, Cook JA, Hillis GS, Walker S, Fraser C, Jia X, Waugh N. 64-Slice computed tomography angiography in the diagnosis and assessment of coronary artery disease: systematic review and meta-analysis. *Heart* 2008; **94**: 1386-1393 [PMID: 18669550 DOI: 10.1136/hrt.2008.145292]

27 **Voros S**, Rinehart S, Qian Z, Joshi P, Vazquez G, Fischer C, Belur P, Hulten E, Villines TC. Coronary atherosclerosis imaging by coronary CT angiography: current status, correlation with intravascular interrogation and meta-analysis. *JACC Cardiovasc Imaging* 2011; **4**: 537-548 [PMID: 21565743 DOI: 10.1016/j.jcmg.2011.03.006]

28 **Villines TC**, Taylor AJ. Multi-ethnic study of atherosclerosis arterial age versus framingham 10-year or lifetime cardiovascular risk. *Am J Cardiol* 2012; **110**: 1627-1630 [PMID: 22921999 DOI: 10.1016/j.amjcard.2012.07.018]

29 **Lee MS**, Chun EJ, Kim KJ, Kim JA, Yoo JY, Choi SI. Asymptomatic subjects with zero coronary calcium score: coronary CT angiographic features of plaques in event-prone patients. *Int J Cardiovasc Imaging* 2013; **29** Suppl 1: 29-36 [PMID: 23754773 DOI: 10.1007/s10554-013-0257-z]

30 **Lin FY**, Shaw LJ, Dunning AM, Labounty TM, Choi JH, Weinsaft JW, Koduru S, Gomez MJ, Delago AJ, Callister TQ, Berman DS, Min JK. Mortality risk in symptomatic patients with nonobstructive coronary artery disease: a prospective 2-center study of 2,583 patients undergoing 64-detector row coronary computed tomographic angiography. *J Am Coll Cardiol* 2011; **58**: 510-519 [PMID: 21777749 DOI: 10.1016/j.jacc.2010.11.078]

31 **Yorgun H**, Canpolat U, Aytemir K, Hazırolan T, Sunman H, Ateş

AH, Sahiner L, Karahan S, Kaya EB, Tokgözoğlu L, Kabakçı G, Oto A. Prognosis of patients with mild-moderate coronary artery stenosis detected by coronary computed tomography angiography. *Int J Cardiol* 2013; **168**: 1195-1200 [PMID: 23201082 DOI: 10.1016/j.ijcard.2012.11.066]

32 **Habib PJ**, Green J, Butterfield RC, Kuntz GM, Murthy R, Kraemer DF, Percy RF, Miller AB, Strom JA. Association of cardiac events with coronary artery disease detected by 64-slice or greater coronary CT angiography: a systematic review and meta-analysis. *Int J Cardiol* 2013; **169**: 112-120 [PMID: 24090745 DOI: 10.1016/j.ijcard.2013.08.096]

33 **Alfonso F**, Salamanca J, Pozo E. Diagnóstico de síndrome coronario agudo en pacientes con dolor torácico en urgencias: ¿cambios a la vista? *Emergencias* 2016; **28**: 6-8

34 **Pozo E**, Álvarez-Acosta L, Alonso D, Pazos-Lopez P, de Siqueira ME, Jacobi A, Narula J, Fuster V, Sanz J. Diagnostic accuracy of coronary ct for the quantification of the syntax score in patients with left main and/or 3-vessel coronary disease. Comparison with invasive angiography. *Int J Cardiol* 2015; **182**: 549-556 [PMID: 25703283 DOI: 10.1016/j.ijcard.2015.01.014]

35 **Wu FZ**, Wu MT. 2014 SCCT guidelines for the interpretation and reporting of coronary CT angiography: a report of the Society of Cardiovascular Computed Tomography Guidelines Committee. *J Cardiovasc Comput Tomogr* 2015; **9**: e3 [PMID: 25708015 DOI: 10.1016/j.jcct.2015.01.003]

36 **Pundziute G**, Schuijf JD, Jukema JW, Decramer I, Sarno G, Vanhoenacker PK, Reiber JH, Schalij MJ, Wijns W, Bax JJ. Head-to-head comparison of coronary plaque evaluation between multislice computed tomography and intravascular ultrasound radiofrequency data analysis. *JACC Cardiovasc Interv* 2008; **1**: 176-182 [PMID: 19463297 DOI: 10.1016/j.jcin.2008.01.007]

37 **Choi BJ**, Kang DK, Tahk SJ, Choi SY, Yoon MH, Lim HS, Kang SJ, Yang HM, Park JS, Zheng M, Hwang GS, Shin JH. Comparison of 64-slice multidetector computed tomography with spectral analysis of intravascular ultrasound backscatter signals for characterizations of noncalcified coronary arterial plaques. *Am J Cardiol* 2008; **102**: 988-993 [PMID: 18929698 DOI: 10.1016/j.amjcard.2008.05.060]

38 **Brodoefel H**, Burgstahler C, Heuschmid M, Reimann A, Khosa F, Kopp A, Schroeder S, Claussen CD, Clouse ME. Accuracy of dual-source CT in the characterisation of non-calcified plaque: use of a colour-coded analysis compared with virtual histology intravascular ultrasound. *Br J Radiol* 2009; **82**: 805-812 [PMID: 19332517 DOI: 10.1259/bjr/35768497]

39 **Otsuka M**, Bruining N, Van Pelt NC, Mollet NR, Ligthart JM, Vourvouri E, Hamers R, De Jaegere P, Wijns W, Van Domburg RT, Stone GW, Veldhof S, Verheye S, Dudek D, Serruys PW, Krestin GP, De Feyter PJ. Quantification of coronary plaque by 64-slice computed tomography: a comparison with quantitative intracoronary ultrasound. *Invest Radiol* 2008; **43**: 314-321 [PMID: 18424952 DOI: 10.1097/RLI.0b013e31816a88a9]

40 **Voros S**, Rinehart S, Qian Z, Vazquez G, Anderson H, Murrieta L, Wilmer C, Carlson H, Taylor K, Ballard W, Karmpaliotis D, Kalynych A, Brown C. Prospective validation of standardized, 3-dimensional, quantitative coronary computed tomographic plaque measurements using radiofrequency backscatter intravascular ultrasound as reference standard in intermediate coronary arterial lesions: results from the ATLANTA (assessment of tissue characteristics, lesion morphology, and hemodynamics by angiography with fractional flow reserve, intravascular ultrasound and virtual histology, and noninvasive computed tomography in atherosclerotic plaques) I study. *JACC Cardiovasc Interv* 2011; **4**: 198-208 [PMID: 21349459 DOI: 10.1016/j.jcin.2010.10.008]

41 **Kashiwagi M**, Tanaka A, Kitabata H, Tsujioka H, Kataiwa H, Komukai K, Tanimoto T, Takemoto K, Takarada S, Kubo T, Hirata K, Nakamura N, Mizukoshi M, Imanishi T, Akasaka T. Feasibility of noninvasive assessment of thin-cap fibroatheroma by multidetector computed tomography. *JACC Cardiovasc Imaging* 2009; **2**: 1412-1419 [PMID: 20083077 DOI: 10.1016/j.jcmg.2009.09.012]

42 **Seifarth H**, Schlett CL, Nakano M, Otsuka F, Károlyi M, Liew G, Maurovich-Horvat P, Alkadhi H, Virmani R, Hoffmann U. Histopathological correlates of the napkin-ring sign plaque in coronary CT angiography. *Atherosclerosis* 2012; **224**: 90-96 [PMID: 22771191 DOI: 10.1016/j.atherosclerosis.2012.06.021]

43 **Ozaki Y**, Okumura M, Ismail TF, Motoyama S, Naruse H, Hattori K, Kawai H, Sarai M, Takagi Y, Ishii J, Anno H, Virmani R, Serruys PW, Narula J. Coronary CT angiographic characteristics of culprit lesions in acute coronary syndromes not related to plaque rupture as defined by optical coherence tomography and angioscopy. *Eur Heart J* 2011; **32**: 2814-2823 [PMID: 21719455 DOI: 10.1093/eurheartj/ehr189]

44 **Motoyama S**, Kondo T, Sarai M, Sugiura A, Harigaya H, Sato T, Inoue K, Okumura M, Ishii J, Anno H, Virmani R, Ozaki Y, Hishida H, Narula J. Multislice computed tomographic characteristics of coronary lesions in acute coronary syndromes. *J Am Coll Cardiol* 2007; **50**: 319-326 [PMID: 17659199 DOI: 10.1016/j.jacc.2007.03.044]

45 **Hernando L**, Corros C, Gonzalo N, Hernández-Antolin R, Bañuelos C, Jiménez-Quevedo P, Bernardo E, Fernández-Ortiz A, Escaned J, Macaya C, Alfonso F. Morphological characteristics of culprit coronary lesions according to clinical presentation: insights from a multimodality imaging approach. *Int J Cardiovasc Imaging* 2013; **29**: 13-21 [PMID: 22527256 DOI: 10.1007/s10554-012-0043-3]

46 **Fujimoto S**, Kondo T, Kodama T, Takase S, Narula J. Delayed plaque enhancement by CT angiography. *JACC Cardiovasc Imaging* 2012; **5**: 1181-1182 [PMID: 23153919 DOI: 10.1016/j.jcmg.2012.01.026]

47 **Hyafil F**, Cornily JC, Feig JE, Gordon R, Vucic E, Amirbekian V, Fisher EA, Fuster V, Feldman LJ, Fayad ZA. Noninvasive detection of macrophages using a nanoparticulate contrast agent for computed tomography. *Nat Med* 2007; **13**: 636-641 [PMID: 17417649 DOI: 10.1038/nm1571]

48 **Motoyama S**, Sarai M, Harigaya H, Anno H, Inoue K, Hara T, Naruse H, Ishii J, Hishida H, Wong ND, Virmani R, Kondo T, Ozaki Y, Narula J. Computed tomographic angiography characteristics of atherosclerotic plaques subsequently resulting in acute coronary syndrome. *J Am Coll Cardiol* 2009; **54**: 49-57 [PMID: 19555840 DOI: 10.1016/j.jacc.2009.02.068]

49 **Otsuka K**, Fukuda S, Tanaka A, Nakanishi K, Taguchi H, Yoshikawa J, Shimada K, Yoshiyama M. Napkin-ring sign on coronary CT angiography for the prediction of acute coronary syndrome. *JACC Cardiovasc Imaging* 2013; **6**: 448-457 [PMID: 23498679 DOI: 10.1016/j.jcmg.2012.09.016]

50 **Versteylen MO**, Kietselaer BL, Dagnelie PC, Joosen IA, Dedic A, Raaijmakers RH, Wildberger JE, Nieman K, Crijns HJ, Niessen WJ, Daemen MJ, Hofstra L. Additive value of semiautomated quantification of coronary artery disease using cardiac computed tomographic angiography to predict future acute coronary syndrome. *J Am Coll Cardiol* 2013; **61**: 2296-2305 [PMID: 23562925 DOI: 10.1016/j.jacc.2013.02.065]

51 **Alfonso F**. Noninvasive detection of vulnerable plaques: are we there yet? *J Am Coll Cardiol* 2010; **55**: 1163; author reply 1163-1164 [PMID: 20223375 DOI: 10.1016/j.jacc.2009.07.076]

52 **Hoffmann U**, Truong QA, Schoenfeld DA, Chou ET, Woodard PK, Nagurney JT, Pope JH, Hauser TH, White CS, Weiner SG, Kalanjian S, Mullins ME, Mikati I, Peacock WF, Zakroysky P, Hayden D, Goehler A, Lee H, Gazelle GS, Wiviott SD, Fleg JL, Udelson JE. Coronary CT angiography versus standard evaluation in acute chest pain. *N Engl J Med* 2012; **367**: 299-308 [PMID: 22830462 DOI: 10.1056/NEJMoa1201161]

53 **Fujimoto S**, Kondo T, Takamura K, Baber U, Shinozaki T, Nishizaki Y, Kawaguchi Y, Matsumori R, Hiki M, Miyauchi K, Daida H, Hecht H, Stone GW, Narula J. Incremental prognostic value of coronary computed tomographic angiography high-risk plaque characteristics in newly symptomatic patients. *J Cardiol* 2016; **67**: 538-544 [PMID: 26359708 DOI: 10.1016/j.jjcc.2015.07.018]

54 **Motoyama S**, Ito H, Sarai M, Kondo T, Kawai H, Nagahara Y, Harigaya H, Kan S, Anno H, Takahashi H, Naruse H, Ishii J,

Hecht H, Shaw LJ, Ozaki Y, Narula J. Plaque Characterization by Coronary Computed Tomography Angiography and the Likelihood of Acute Coronary Events in Mid-Term Follow-Up. *J Am Coll Cardiol* 2015; **66**: 337-346 [PMID: 26205589 DOI: 10.1016/j.jacc.2015.05.069]

55   **Kodama T**, Kondo T, Oida A, Fujimoto S, Narula J. Computed tomographic angiography-verified plaque characteristics and slow-flow phenomenon during percutaneous coronary intervention. *JACC Cardiovasc Interv* 2012; **5**: 636-643 [PMID: 22721658 DOI: 10.1016/j.jcin.2012.02.016]

56   **Inoue K**, Motoyama S, Sarai M, Sato T, Harigaya H, Hara T, Sanda Y, Anno H, Kondo T, Wong ND, Narula J, Ozaki Y. Serial coronary CT angiography-verified changes in plaque characteristics as an end point: evaluation of effect of statin intervention. *JACC Cardiovasc Imaging* 2010; **3**: 691-698 [PMID: 20633846 DOI: 10.1016/j.jcmg.2010.04.011]

57   **Brodoefel H**, Reimann A, Heuschmid M, Tsiflikas I, Kopp AF, Schroeder S, Claussen CD, Clouse ME, Burgstahler C. Characterization of coronary atherosclerosis by dual-source computed tomography and HU-based color mapping: a pilot study. *Eur Radiol* 2008; **18**: 2466-2474 [PMID: 18491107 DOI: 10.1007/s00330-008-1019-5]

58   **Hur J**, Kim YJ, Lee HJ, Nam JE, Choe KO, Seo JS, Choi DH, Kim JS, Choi BW. Quantification and characterization of obstructive coronary plaques using 64-slice computed tomography: a comparison with intravascular ultrasound. *J Comput Assist Tomogr* 2009; **33**: 186-192 [PMID: 19346843 DOI: 10.1097/RCT.0b013e31817c420f]

59   **Sun J**, Zhang Z, Lu B, Yu W, Yang Y, Zhou Y, Wang Y, Fan Z. Identification and quantification of coronary atherosclerotic plaques: a comparison of 64-MDCT and intravascular ultrasound. *AJR Am J Roentgenol* 2008; **190**: 748-754 [PMID: 18287448 DOI: 10.2214/AJR.07.2763]

60   **Obaid DR**, Calvert PA, Gopalan D, Parker RA, West NE, Goddard M, Rudd JH, Bennett MR. Dual-energy computed tomography imaging to determine atherosclerotic plaque composition: a prospective study with tissue validation. *J Cardiovasc Comput Tomogr* 2014; **8**: 230-237 [PMID: 24939072 DOI: 10.1016/j.jcct.2014.04.007]

61   **Hendel RC**, Patel MR, Kramer CM, Poon M, Hendel RC, Carr JC, Gerstad NA, Gillam LD, Hodgson JM, Kim RJ, Kramer CM, Lesser JR, Martin ET, Messer JV, Redberg RF, Rubin GD, Rumsfeld JS, Taylor AJ, Weigold WG, Woodard PK, Brindis RG, Hendel RC, Douglas PS, Peterson ED, Wolk MJ, Allen JM, Patel MR. ACCF/ACR/SCCT/SCMR/ASNC/NASCI/SCAI/SIR 2006 appropriateness criteria for cardiac computed tomography and cardiac magnetic resonance imaging: a report of the American College of Cardiology Foundation Quality Strategic Directions Committee Appropriateness Criteria Working Group, American College of Radiology, Society of Cardiovascular Computed Tomography, Society for Cardiovascular Magnetic Resonance, American Society of Nuclear Cardiology, North American Society for Cardiac Imaging, Society for Cardiovascular Angiography and Interventions, and Society of Interventional Radiology. *J Am Coll Cardiol* 2006; **48**: 1475-1497 [PMID: 17010819 DOI: 10.1016/j.jacc.2006.07.003]

62   **Mahrholdt H**, Wagner A, Judd RM, Sechtem U, Kim RJ. Delayed enhancement cardiovascular magnetic resonance assessment of non-ischaemic cardiomyopathies. *Eur Heart J* 2005; **26**: 1461-1474 [PMID: 15831557 DOI: 10.1093/eurheartj/ehi258]

63   **Sharma V**, Binukrishnan S, Schoepf UJ, Ruzsics B. Myocardial tissue characterization with magnetic resonance imaging. *J Thorac Imaging* 2014; **29**: 318-330 [PMID: 24394716 DOI: 10.1097/RTI.0000000000000053]

64   **Hamdan A**, Asbach P, Wellnhofer E, Klein C, Gebker R, Kelle S, Kilian H, Huppertz A, Fleck E. A prospective study for comparison of MR and CT imaging for detection of coronary artery stenosis. *JACC Cardiovasc Imaging* 2011; **4**: 50-61 [PMID: 21232704 DOI: 10.1016/j.jcmg.2010.10.007]

65   **Yang Q**, Li K, Liu X, Bi X, Liu Z, An J, Zhang A, Jerecic R, Li D. Contrast-enhanced whole-heart coronary magnetic resonance angiography at 3.0-T: a comparative study with X-ray angiography in a single center. *J Am Coll Cardiol* 2009; **54**: 69-76 [PMID: 19555843 DOI: 10.1016/j.jacc.2009.03.016]

66   **Scott AD**, Keegan J, Firmin DN. Motion in cardiovascular MR imaging. *Radiology* 2009; **250**: 331-351 [PMID: 19188310 DOI: 10.1148/radiol.2502071998]

67   **Stuber M**, Botnar RM, Danias PG, Sodickson DK, Kissinger KV, Van Cauteren M, De Becker J, Manning WJ. Double-oblique free-breathing high resolution three-dimensional coronary magnetic resonance angiography. *J Am Coll Cardiol* 1999; **34**: 524-531 [PMID: 10440168]

68   **Lustig M**, Donoho D, Pauly JM. Sparse MRI: The application of compressed sensing for rapid MR imaging. *Magn Reson Med* 2007; **58**: 1182-1195 [PMID: 17969013 DOI: 10.1002/mrm.21391]

69   **Pruessmann KP**, Weiger M, Scheidegger MB, Boesiger P. SENSE: sensitivity encoding for fast MRI. *Magn Reson Med* 1999; **42**: 952-962 [PMID: 10542355]

70   **Fischer SE**, Wickline SA, Lorenz CH. Novel real-time R-wave detection algorithm based on the vectorcardiogram for accurate gated magnetic resonance acquisitions. *Magn Reson Med* 1999; **42**: 361-370 [PMID: 10440961]

71   **Henningsson M**, Koken P, Stehning C, Razavi R, Prieto C, Botnar RM. Whole-heart coronary MR angiography with 2D self-navigated image reconstruction. *Magn Reson Med* 2012; **67**: 437-445 [PMID: 21656563 DOI: 10.1002/mrm.23027]

72   **Meyer CH**, Hu BS, Nishimura DG, Macovski A. Fast spiral coronary artery imaging. *Magn Reson Med* 1992; **28**: 202-213 [PMID: 1461123]

73   **Stehning C**, Börnert P, Nehrke K, Eggers H, Stuber M. Free-breathing whole-heart coronary MRA with 3D radial SSFP and self-navigated image reconstruction. *Magn Reson Med* 2005; **54**: 476-480 [PMID: 16032682 DOI: 10.1002/mrm.20557]

74   **Hu P**, Chan J, Ngo LH, Smink J, Goddu B, Kissinger KV, Goepfert L, Hauser TH, Rofsky NM, Manning WJ, Nezafat R. Contrast-enhanced whole-heart coronary MRI with bolus infusion of gadobenate dimeglumine at 1.5 T. *Magn Reson Med* 2011; **65**: 392-398 [PMID: 21264933 DOI: 10.1002/mrm.22706]

75   **Nagata M**, Kato S, Kitagawa K, Ishida N, Nakajima H, Nakamori S, Ishida M, Miyahara M, Ito M, Sakuma H. Diagnostic accuracy of 1.5-T unenhanced whole-heart coronary MR angiography performed with 32-channel cardiac coils: initial single-center experience. *Radiology* 2011; **259**: 384-392 [PMID: 21406635 DOI: 10.1148/radiol.11101323]

76   **Gerretsen S**, Kessels AG, Nelemans PJ, Dijkstra J, Reiber JH, van der Geest RJ, Katoh M, Waltenberger J, van Engelshoven JM, Botnar RM, Kooi ME, Leiner T. Detection of coronary plaques using MR coronary vessel wall imaging: validation of findings with intravascular ultrasound. *Eur Radiol* 2013; **23**: 115-124 [PMID: 22782568 DOI: 10.1007/s00330-012-2576-1]

77   **He Y**, Zhang Z, Dai Q, Zhou Y, Yang Y, Yu W, An J, Jin L, Jerecic R, Yuan C, Li D. Accuracy of MRI to identify the coronary artery plaque: a comparative study with intravascular ultrasound. *J Magn Reson Imaging* 2012; **35**: 72-78 [PMID: 21989946 DOI: 10.1002/jmri.22652]

78   **Botnar RM**. Coronary plaque characterization by T(1)-weighted cardiac magnetic resonance. *JACC Cardiovasc Imaging* 2009; **2**: 729-730 [PMID: 19520343 DOI: 10.1016/j.jcmg.2009.04.002]

79   **Yeon SB**, Sabir A, Clouse M, Martinezclark PO, Peters DC, Hauser TH, Gibson CM, Nezafat R, Maintz D, Manning WJ, Botnar RM. Delayed-enhancement cardiovascular magnetic resonance coronary artery wall imaging: comparison with multislice computed tomography and quantitative coronary angiography. *J Am Coll Cardiol* 2007; **50**: 441-447 [PMID: 17662397 DOI: 10.1016/j.jacc.2007.03.052]

80   **Jansen CH**, Perera D, Makowski MR, Wiethoff AJ, Phinikaridou A, Razavi RM, Marber MS, Greil GF, Nagel E, Maintz D, Redwood S, Botnar RM. Detection of intracoronary thrombus by magnetic resonance imaging in patients with acute myocardial infarction. *Circulation* 2011; **124**: 416-424 [PMID: 21747055 DOI: 10.1161/CIRCULATIONAHA.110.965442]

81 **Ehara S**, Hasegawa T, Nakata S, Matsumoto K, Nishimura S, Iguchi T, Kataoka T, Yoshikawa J, Yoshiyama M. Hyperintense plaque identified by magnetic resonance imaging relates to intracoronary thrombus as detected by optical coherence tomography in patients with angina pectoris. *Eur Heart J Cardiovasc Imaging* 2012; **13**: 394-399 [PMID: 22277117 DOI: 10.1093/ehjci/jer305]

82 **Kawasaki T**, Koga S, Koga N, Noguchi T, Tanaka H, Koga H, Serikawa T, Orita Y, Ikeda S, Mito T, Goto Y, Shintani Y, Tanaka A, Fukuyama T. Characterization of hyperintense plaque with noncontrast T(1)-weighted cardiac magnetic resonance coronary plaque imaging: comparison with multislice computed tomography and intravascular ultrasound. *JACC Cardiovasc Imaging* 2009; **2**: 720-728 [PMID: 19520342 DOI: 10.1016/j.jcmg.2009.01.016]

83 **Noguchi T**, Kawasaki T, Tanaka A, Yasuda S, Goto Y, Ishihara M, Nishimura K, Miyamoto Y, Node K, Koga N. High-intensity signals in coronary plaques on noncontrast T1-weighted magnetic resonance imaging as a novel determinant of coronary events. *J Am Coll Cardiol* 2014; **63**: 989-999 [PMID: 24345595 DOI: 10.1016/j.jacc.2013.11.034]

84 **Noguchi T**, Tanaka A, Kawasaki T, Goto Y, Morita Y, Asaumi Y, Nakao K, Fujiwara R, Nishimura K, Miyamoto Y, Ishihara M, Ogawa H, Koga N, Narula J, Yasuda S. Effect of Intensive Statin Therapy on Coronary High-Intensity Plaques Detected by Noncontrast T1-Weighted Imaging: The AQUAMARINE Pilot Study. *J Am Coll Cardiol* 2015; **66**: 245-256 [PMID: 26184618 DOI: 10.1016/j.jacc.2015.05.056]

85 **Kim WY**, Christiansen EH, Thrysøe SA, Al-Mashhadi RH, Bøtker HE, Bøttcher M, Holm NR, Falk E. First in vivo demonstration of coronary edema in culprit lesion of patient with acute coronary syndrome by cardiovascular magnetic resonance. *Circ Cardiovasc Imaging* 2011; **4**: 344-346 [PMID: 21586745 DOI: 10.1161/CIRCIMAGING.110.963074]

86 **Pedersen SF**, Thrysøe SA, Paaske WP, Thim T, Falk E, Ringgaard S, Kim WY. Determination of edema in porcine coronary arteries by T2 weighted cardiovascular magnetic resonance. *J Cardiovasc Magn Reson* 2011; **13**: 52 [PMID: 21936914 DOI: 10.1186/1532-429X-13-52]

87 **Ibrahim T**, Makowski MR, Jankauskas A, Maintz D, Karch M, Schachoff S, Manning WJ, Schömig A, Schwaiger M, Botnar RM. Serial contrast-enhanced cardiac magnetic resonance imaging demonstrates regression of hyperenhancement within the coronary artery wall in patients after acute myocardial infarction. *JACC Cardiovasc Imaging* 2009; **2**: 580-588 [PMID: 19442944 DOI: 10.1016/j.jcmg.2008.12.029]

88 **Botnar RM**, Perez AS, Witte S, Wiethoff AJ, Laredo J, Hamilton J, Quist W, Parsons EC, Vaidya A, Kolodziej A, Barrett JA, Graham PB, Weisskoff RM, Manning WJ, Johnstone MT. In vivo molecular imaging of acute and subacute thrombosis using a fibrin-binding magnetic resonance imaging contrast agent. *Circulation* 2004; **109**: 2023-2029 [PMID: 15066940 DOI: 10.1161/01.CIR.0000127034.50006.C0]

89 **Flacke S**, Fischer S, Scott MJ, Fuhrhop RJ, Allen JS, McLean M, Winter P, Sicard GA, Gaffney PJ, Wickline SA, Lanza GM. Novel MRI contrast agent for molecular imaging of fibrin: implications for detecting vulnerable plaques. *Circulation* 2001; **104**: 1280-1285 [PMID: 11551880]

90 **Spuentrup E**, Botnar RM, Wiethoff AJ, Ibrahim T, Kelle S, Katoh M, Ozgun M, Nagel E, Vymazal J, Graham PB, Günther RW, Maintz D. MR imaging of thrombi using EP-2104R, a fibrin-specific contrast agent: initial results in patients. *Eur Radiol* 2008; **18**: 1995-2005 [PMID: 18425519 DOI: 10.1007/s00330-008-0965-2]

91 **Makowski MR**, Wiethoff AJ, Blume U, Cuello F, Warley A, Jansen CH, Nagel E, Razavi R, Onthank DC, Cesati RR, Marber MS, Schaeffter T, Smith A, Robinson SP, Botnar RM. Assessment of atherosclerotic plaque burden with an elastin-specific magnetic resonance contrast agent. *Nat Med* 2011; **17**: 383-388 [PMID: 21336283 DOI: 10.1038/nm.2310]

92 **Sirol M**, Itskovich VV, Mani V, Aguinaldo JG, Fallon JT, Misselwitz B, Weinmann HJ, Fuster V, Toussaint JF, Fayad ZA. Lipid-rich atherosclerotic plaques detected by gadofluorine-enhanced in vivo magnetic resonance imaging. *Circulation* 2004; **109**: 2890-2896 [PMID: 15184290 DOI: 10.1161/01.CIR.0000129310.17277.E7]

93 **Ronald JA**, Chen Y, Belisle AJ, Hamilton AM, Rogers KA, Hegele RA, Misselwitz B, Rutt BK. Comparison of gadofluorine-M and Gd-DTPA for noninvasive staging of atherosclerotic plaque stability using MRI. *Circ Cardiovasc Imaging* 2009; **2**: 226-234 [PMID: 19808597 DOI: 10.1161/CIRCIMAGING.108.826826]

94 **Lobbes MB**, Heeneman S, Passos VL, Welten R, Kwee RM, van der Geest RJ, Wiethoff AJ, Caravan P, Misselwitz B, Daemen MJ, van Engelshoven JM, Leiner T, Kooi ME. Gadofosveset-enhanced magnetic resonance imaging of human carotid atherosclerotic plaques: a proof-of-concept study. *Invest Radiol* 2010; **45**: 275-281 [PMID: 20351652 DOI: 10.1097/RLI.0b013e3181d5466b]

95 **Pedersen SF**, Thrysøe SA, Paaske WP, Thim T, Falk E, Ringgaard S, Kim WY. CMR assessment of endothelial damage and angiogenesis in porcine coronary arteries using gadofosveset. *J Cardiovasc Magn Reson* 2011; **13**: 10 [PMID: 21269470 DOI: 10.1186/1532-429X-13-10]

96 **Phinikaridou A**, Andia ME, Protti A, Indermuehle A, Shah A, Smith A, Warley A, Botnar RM. Noninvasive magnetic resonance imaging evaluation of endothelial permeability in murine atherosclerosis using an albumin-binding contrast agent. *Circulation* 2012; **126**: 707-719 [PMID: 22753191 DOI: 10.1161/CIRCULATIONAHA.112.092098]

97 **Alam SR**, Shah AS, Richards J, Lang NN, Barnes G, Joshi N, MacGillivray T, McKillop G, Mirsadraee S, Payne J, Fox KA, Henriksen P, Newby DE, Semple SI. Ultrasmall superparamagnetic particles of iron oxide in patients with acute myocardial infarction: early clinical experience. *Circ Cardiovasc Imaging* 2012; **5**: 559-565 [PMID: 22875883 DOI: 10.1161/CIRCIMAGING.112.974907]

98 **Rudd JH**, Hyafil F, Fayad ZA. Inflammation imaging in atherosclerosis. *Arterioscler Thromb Vasc Biol* 2009; **29**: 1009-1016 [PMID: 19304673 DOI: 10.1161/ATVBAHA.108.165563]

99 **Sanz J**, Fayad ZA. Imaging of atherosclerotic cardiovascular disease. *Nature* 2008; **451**: 953-957 [PMID: 18288186 DOI: 10.1038/nature06803]

100 **Wykrzykowska J**, Lehman S, Williams G, Parker JA, Palmer MR, Varkey S, Kolodny G, Laham R. Imaging of inflamed and vulnerable plaque in coronary arteries with 18F-FDG PET/CT in patients with suppression of myocardial uptake using a low-carbohydrate, high-fat preparation. *J Nucl Med* 2009; **50**: 563-568 [PMID: 19289431 DOI: 10.2967/jnumed.108.055616]

101 **Alexanderson E**, Slomka P, Cheng V, Meave A, Saldaña Y, García-Rojas L, Berman D. Fusion of positron emission tomography and coronary computed tomographic angiography identifies fluorine 18 fluorodeoxyglucose uptake in the left main coronary artery soft plaque. *J Nucl Cardiol* 2008; **15**: 841-843 [PMID: 18984461 DOI: 10.1007/BF03007367]

102 **Rogers IS**, Nasir K, Figueroa AL, Cury RC, Hoffmann U, Vermylen DA, Brady TJ, Tawakol A. Feasibility of FDG imaging of the coronary arteries: comparison between acute coronary syndrome and stable angina. *JACC Cardiovasc Imaging* 2010; **3**: 388-397 [PMID: 20394901 DOI: 10.1016/j.jcmg.2010.01.004]

103 **Dweck MR**, Chow MW, Joshi NV, Williams MC, Jones C, Fletcher AM, Richardson H, White A, McKillop G, van Beek EJ, Boon NA, Rudd JH, Newby DE. Coronary arterial 18F-sodium fluoride uptake: a novel marker of plaque biology. *J Am Coll Cardiol* 2012; **59**: 1539-1548 [PMID: 22516444 DOI: 10.1016/j.jacc.2011.12.037]

104 **Gaemperli O**, Shalhoub J, Owen DR, Lamare F, Johansson S, Fouladi N, Davies AH, Rimoldi OE, Camici PG. Imaging intraplaque inflammation in carotid atherosclerosis with 11C-PK11195 positron emission tomography/computed tomography. *Eur Heart J* 2012; **33**: 1902-1910 [PMID: 21933781 DOI: 10.1093/eurheartj/ehr367]

105 **Rominger A**, Saam T, Vogl E, Ubleis C, la Fougère C, Förster S, Haug A, Cumming P, Reiser MF, Nikolaou K, Bartenstein P, Hacker M. In vivo imaging of macrophage activity in the coronary arteries using 68Ga-DOTATATE PET/CT: correlation with coronary calcium burden and risk factors. *J Nucl Med* 2010; **51**: 193-197 [PMID: 20080898 DOI: 10.2967/jnumed.109.070672]

106 **Asaumi Y**, Noguchi T, Morita Y, Matsuyama TA, Otsuka F,

Fujiwara R, Kanaya T, Nagai T, Higashi M, Kusano K, Anzai T, Ishibashi-Ueda H, Ogawa H, Yasuda S. Non-contrast T1-weighted magnetic resonance imaging at 3.0 Tesla in a patient undergoing elective percutaneous coronary intervention – clinical and pathological significance of high-intensity plaque. *Circ J* 2015; **79**: 218-220 [PMID: 25342532 DOI: 10.1253/circj.CJ-14-0897]

107   **Cheng VY**, Slomka PJ, Le Meunier L, Tamarappoo BK, Nakazato R, Dey D, Berman DS. Coronary arterial 18F-FDG uptake by fusion of PET and coronary CT angiography at sites of percutaneous stenting for acute myocardial infarction and stable coronary artery disease. *J Nucl Med* 2012; **53**: 575-583 [PMID: 22419753 DOI: 10.2967/jnumed.111.097550]